Ab initio study of ground and excited states of NiO(100) monolayer

2000 J. Phys.: Condens. Matter 12 2163

(http://iopscience.iop.org/0953-8984/12/10/303)

J. Phys.: Condens. Matter **12** (2000) 2163–2181. Printed in the UK PII: S0953-8984(00)07312-4

Ab initio study of ground and excited states of NiO(100) monolayer

Claudine Noguera† and W C Mackrodt‡

† Laboratoire de Physique des Solides, Associé au CNRS, Université Paris Sud, 91405 Orsay, France

‡ School of Chemistry, University of St Andrews, St Andrews, Fife KY16 9ST, UK

E-mail: wcm@st-and.ac.uk (W C Mackrodt)

Received 31 August 1999

Abstract. *Ab initio* periodic Hartree–Fock calculations are reported of ground and d $\rightarrow$ d excited states of an *unsupported* NiO(100) *monolayer* in the ferromagnetic, ferrimagnetic, antiferromagnetic and fully frustrated spin alignments as a function of the lattice constant. The ground state is found to be highly ionic and insulating with a minimum energy lattice constant of 4.0 Å. The Ni(d^8) configuration is $[(xz)^2(yz)^2(xy)^2(z^2)^1(x^2-y^2)^1]$, as found previously for the bulk, despite the reduced dimensionality leading to a reduction in the number of nearest neighbours and difference in the ligand-field ordering. The valence band DOS resembles closely that of the bulk with a majority weight of O(p) states at the upper edge leading to a charge-transfer system. The Ni d states occur $\sim$1 eV below the O(p) band and are dispersed over $\sim$4.5 eV in three distinct sub-bands. The relative stability of the four spin alignments is antiferromagnetic > ferrimagnetic > ferromagnetic > fully frustrated, with differences in energy of 10.779 meV, 10.017 meV and 1.675 meV respectively at 4.0 Å. Values of -0.84 meV and -10.78 meV can be deduced for the direct spin–spin, E_d, and superexchange, E_{se}, interaction energies respectively, which compare with values of -1.5 meV and -7.0 meV found previously for the bulk at a lattice constant of 4.265 Å. E_{se} is found to decrease rapidly to -3.66 meV at 4.5 Å, unlike E_d which remains fairly constant. This reduction in E_{se} is attributed largely to the increase in the band gap of the monolayer compared with the bulk. For the ferromagnetic spin alignment at 4.0 Å variationally converged solutions have been obtained for the one-electron $d_{xy} \rightarrow d_{z^2}$, $d_{xy} \rightarrow d_{x^2-y^2}$ and spin-forbidden $d_{x^2-y^2} \rightarrow d_{z^2}$ excited states and the two-electron $d_{xy}/d_{yz} \rightarrow d_{z^2}/d_{x^2-y^2}$ excited state with excitation energies of 1.16 eV, 1.09 eV, 1.84 eV and 1.79 eV respectively. These are close to values that have been deduced from optical and EEL spectra and high-level cluster calculations. Converged solutions for the $d_{xy} \rightarrow d_{z^2}$ excited state in the ferromagnetic alignment have been obtained for the concentration range 1–4 excited states per 2×2 unit cell and in the other spin alignments for complete excitation at lattice constants from 3.9 to 5.0 Å. These show $d_{xy} \rightarrow d_{z^2}$ excitations, and by implication other d $\rightarrow$ d excitations, to be highly local with an interaction energy of < 0.1 eV per excitation at saturation, to be independent of the spin alignment and to increase slightly with lattice constant. The favourable arrangement of the nearest neighbour unpaired spins in the $d_{xy} \rightarrow d_{z^2}$ excited state leads to values of E_d, the direct spin–spin coupling energy, which are an order of magnitude greater than the ground state values and appreciably in excess of the bulk value. E_{se}, on the other hand, remains approximately the same. The first ionized state is found to be essentially $d^8\underline{L}$, as it is in the bulk, with strong localization of the hole in a p_π orbital of a single O atom and retention of the local Ni moments. By direct analogy with the changes in the oxygen k-edge spectrum of $Li_xNi_{1-x}O$ the band gap in the NiO(100) monolayer is estimated to be $\sim$5.3 eV from the gap between the hole band and the conduction band edge. The first electron addition state is found to be essentially $d^9[(d_{z^2})^2]$. The energy of the single charge-transfer excitonic state of a 2×2 unit cell is estimated to be to be $\sim$5.6 eV, in close agreement with the band gap deduced from the DOS of the first ionized state.

0953-8984/00/102163+19$30.00

1. Introduction

Over the past few years, important advances have been made in the fabrication of ultra-thin crystalline oxide layers grown epitaxially on a variety of substrates [1]. The methods which are commonly used are direct oxidation of a metallic surface or deposition of metal atoms followed by controlled oxidation. In this way, films a few Ångströms thick may be grown, the crystallinity and perfection of which depend strongly on the ratio of the lattice parameter of the oxide to that of the substrate and details of the preparative conditions such as deposition rate, oxidizing temperature etc. These ultra-thin films exhibit several unusual properties which are of interest both from a fundamental point of view [2–4] and with regard to potential technological application. First, as a result of their small thickness, they do not charge when exposed to electron or electromagnetic radiation and can thus be submitted to detailed spectroscopic investigation. They may also exhibit surfaces which are not usually obtained by direct cleavage of the bulk, which is the case for high energy surface orientations such as polar surfaces. The constraint imposed by the substrate may also lead these epitaxial oxide layers to adopt lattice symmetries which differ from those of the thermodynamically stable bulk, and, where structural phase transitions occur, transition temperatures can depend strongly on the thickness of the epitaxial layer.

It is within this context that we have initiated a theoretical study of ultra-thin films and nanostructures of NiO. NiO is a paradigm magnetic insulator whose bulk and surface properties have been the subject of extensive experimental and theoretical investigation [5]. It has long been considered as highly ionic and early first principles calculations based on the local spin density approximation (LSD) described it as a Mott–Hubbard system in the AF_2 spin arrangement with a narrow gap spanned by Ni d-states [6]. However, seminal work by Sawatzky *et al* [7–9] showed that hole states in Li:NiO were largely of O(p) character which suggested that the first ionized state of NiO is essentially $d^8\underline{L}$ and the ground state of $p \rightarrow d$ charge-transfer type. Subsequent first principles calculations have confirmed the majority weight of the valence band edge to be O(p), including spin unrestricted periodic Hartree–Fock (UHF) calculations [10–12]. The latter have shown that the insulating and (high spin) magnetic properties are the result of large on-site Coulomb and exchange interactions between essentially localized electrons with strong orbital polarization resulting from the orbital dependence of the one-electron potential. This is determined principally by the non-local exchange interaction which is evaluated exactly within the Hartree–Fock approximation and implemented, again exactly, in the CRYSTAL code [13]. UHF calculations have also confirmed the AF_2 spin arrangement by direct comparisons with F and AF_1 total energies, predicted spin–lattice distortion of the AF_2 structure in good agreement with experiment [10] and provided direct evidence of O(p) holes in Li:NiO [14] and NiO [15] and Fe(d) holes in Fe:NiO [15], again, in agreement with experiment [16]. Thus, despite its approximate nature and inherent limitations, the *periodic* UHF method would seem to be well suited to describing NiO in lower dimensions, and here we report calculations, we believe for the first time, of the ground and excited states of a *single unsupported* {100} layer of NiO, in which Ni is fourfold coordinated. Included in this study are d–d excitation energies obtained *directly* from total energy differences, the magnetism of d–d excited states, the interaction energy of d–d excitons and the variation of d–d excitation energy with lattice constant, charge-transfer exciton formation and condensation energies, a comparison of band gaps derived from total energy differences and single particle eigenvalues, a comparison of the potential energy surfaces of ground and charge transfer states as a function of lattice constant and the magnetism of the first ionized state.

The calculations reported here are a first step towards a systematic analysis of the effects of coordination on the electronic and magnetic properties of ground and excited states of NiO and

are a prelude to further studies of ultra-thin films and nanostructures in which we will determine the extent to which they are representative of deposited monolayers by examining, in detail, the influence of the physical and chemical structure of the substrate. While there appear to be no other calculations based on extended/periodic systems for comparison, there have been *cluster* calculations at and beyond the Hartree–Fock level which have attempted to simulate the bulk and {100} surface with six- and fivefold coordination of Ni respectively. They have included studies of magnetic interactions [17] and both d $\rightarrow$ d [18–20] and charge-transfer [20] excitations and provide a guide as to the influence of electron correlation. However, it is clear that non-local effects play an important role in solids, notably in polaron formation, colour centre stability and other defect phenomena where long-range lattice polarization makes a significant contribution [21], in magnetic effects of the type reported recently by Alders *et al* [4] in epitaxial layers of varying thickness and in chemical and physical effects of substrates [22–24].

In section 2 we review briefly the theoretical methods used and in section 3 present the main body of our results, which we discuss in section 4.

2. Theoretical methods

The all-electron *ab initio* LCAO Hartree–Fock method for periodic systems and its computational implementation in the CRYSTAL 95 computer code [13] have been described in detail previously [25]. The calculations reported here use extended Gaussian basis sets and are based on the spin unrestricted (UHF) procedure [26] to describe open-shell electronic configurations. The numerical values of the tolerance parameters involved in the evaluation of the (infinite) Coulomb and exchange series were identical to those used in recent studies [10, 11, 14, 15]: a detailed account of the effect of these tolerances is discussed elsewhere [27]. The reciprocal space integration utilized the Monkhorst–Pack sampling [28], with shrinking factors that gave 15–36 k-points in the IBZ, depending on the overall symmetry of the calculation, and the SCF convergence criterion based on differences in the total energy of the unit cell of less than 10^{-6} Ha. As in previous calculations for the bulk [10, 11, 14, 15], the localized crystal orbitals consisted of 25 atomic orbitals for Ni and 14 for O the type

Ni : 1s(8)2sp(6)3sp(4)4sp(1)5sp(1)3d(4)4d(1) O : 1s(8)2sp(4)3sp(1)4sp(1)

where the numbers in brackets are the numbers of Gaussian functions used to describe the corresponding shell, e.g. 1s, 2sp, 3d etc. The exponents and contraction coefficients were identical to those used for the bulk [10, 11, 14, 15].

To investigate the magnetic properties of monolayer NiO(100), we have considered four spin arrangements of a 2 $\times$ 2 unit cell shown below,

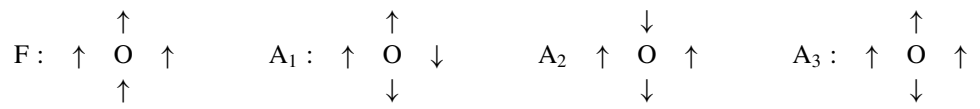

where $\uparrow$ and $\downarrow$ represent high spin Ni^{2+} ions and F, A_1, A_2 and A_3 the ferromagnetic, antiferromagnetic, fully frustrated and ferrimagnetic spin alignments respectively. As described in detail below, in addition to the ground state we have obtained converged UHF solutions for a number of local d $\rightarrow$ d excited states involving single and multiple (N) excitations, which we designate as e_N. Thus, by an '$e_4\, d_{xy} \rightarrow d_{z^2}$ excited state', for example, we mean a state in which all four Ni ions of the 2 $\times$ 2 unit cell have undergone a $d_{xy} \rightarrow d_{z^2}$ excitation. We have also obtained converged UHF solutions for the $d^8p^6 \rightarrow d^9p^5$ charge

transfer state, from which we derive estimates of the band gap and Mott–Wannier exciton condensation energies.

Our treatment of the free hole and electron follows that previously used for the bulk [15], wherein a renormalization of the (infinite) inter-cell Coulombic interaction is effected by adding a uniform background charge of opposite sign and equal magnitude to the crystal potential in the plane of the monolayer. As our results indicate, this has no effect on the densities of states, other than a rigid shift in energy of the single particle spectrum. Furthermore, we confine our attention to *differences* in total energy only, as between various electronic and spin states of the hole, which, again, are invariant to the uniform background charge.

3. Results

3.1. Ground states

We begin with a brief resumé of bulk NiO [10], which UHF calculations predict to be a highly ionic, high spin, p $\rightarrow$ d charge transfer insulator with a lattice constant of $\sim$4.265 Å. The d^8 ground state configuration is

$$[(t_{2g})^6(e_g)^2] \equiv [(d_{xz})^2(d_{yz})^2(d_{xy})^2(d_{z^2})^1(d_{x^2-y^2})^1]$$

with

$$\varepsilon(e_g)_\alpha < \varepsilon(t_{2g})_\alpha < \varepsilon(t_{2g})_\beta < \varepsilon(e_g)_\beta$$

where the subscripts α and β refer to spin up ($\uparrow$) and spin down ($\downarrow$) electrons respectively.

A simple Brandow analysis [29] gives

$$\varepsilon(t_{2g})_\alpha - \varepsilon(e_g)_\alpha = 2J - 10D_q$$
$$\varepsilon(t_{2g})_\beta - \varepsilon(t_{2g})_\alpha = 2J$$
$$\varepsilon(e_g)_\beta - \varepsilon(t_{2g})_\beta = U - 3J + 10D_q$$

where U, J and $10D_q$ are the on-site Coulomb and exchange energies and crystal field splitting. Values of 27.92 eV, 1.01 eV and 0.33 eV respectively are obtained from the appropriate integrals or more approximate values of 26.04 eV, 1.06 eV and 0.73 eV from the calculated band structure at the Γ point [10]. In particular, this analysis shows that the splitting of the $\varepsilon(t_{2g})_\alpha - \varepsilon(e_g)_\alpha$ states depends on the difference, $(2J - 10D_q)$, which UHF calculations find to be positive for the ground state of NiO. The local Ni spin magnetic moment is calculated to be $\sim$1.9 μ_B and the stability of low index spin alignments,

$$AF_2 > F > AF_1$$

below the Néel temperature [10]. If, to a first approximation, it is assumed that the differences in energy, per Ni atom, between the AF_2, F and AF_1 alignments can be written simply in terms of direct spin–spin (d) and indirect super-exchange (se) interactions as

$$E(F) = B + 6\tilde{E}_d$$
$$E(AF_1) = B + 2\tilde{E}_d$$
$$E(AF_2) = B + 3(\tilde{E}_d + \tilde{E}_{se})$$

where B is a constant, UHF total energies lead to values of -1.5 meV and -7.0 meV for $\tilde{E}_d$ and $\tilde{E}_{se}$ respectively. From an analysis of the unoccupied O(p) density of states (DOS) of both Li:NiO [14] and the self-trapped hole in NiO [11], the band gap is estimated to be $\sim$4 eV, which is in the vicinity of the most recent experimental values [5].

Turning now to monolayer NiO(100), we have obtained converged UHF solutions of the ground electronic states of the F, A_1, A_2 and A_3 spin alignments as a function of the

lattice constant, a_0. Of these, the A_1 spin alignment is the most stable for the whole range of values of a_0 with a minimum energy close to 4.0 Å. In this region, Mulliken analyses [30] yield effective atomic charges of $\sim$1.9 e, 3d populations of $\sim$8.1 and local spin moments of $\sim$1.9 μ_B, all of which indicate that the highly ionic, high spin character of the bulk is retained in two dimensions. Furthermore, the high spin d^8 ground state configuration, $[(d_{xz})^2(d_{yz})^2(d_{xy})^2(d_{z^2})^1(d_{x^2-y^2})^1]$ with (100) $\equiv xy$ plane and Ni–O bonds along the x and y axes, is found to remain unchanged from the bulk in all four spin alignments, the stabilities of which are in the order

$$A_1 > A_3 > F > A_2$$

for values of the lattice constant up to, and in excess of, 5 Å, as shown in table 1.

Table 1. Energies (meV/Ni) of the ground states of the A_3, F and A_2 configurations relative to A_1, as a function of a_0 (Å).

a_0 (Å)	A_3	F	A_2
3.9	13.506	26.566	27.638
4.0	10.779	20.796	22.471
4.1	8.587	16.163	18.146
4.2	6.866	12.781	14.748
4.2646	5.947	10.985	12.961
4.3	5.529	10.072	12.043
4.5	3.661	6.242	8.121
5.0	1.413	1.850	3.516

As in the case of the bulk, the relative energies of A_1, A_2, A_3 and F can be written to a first approximation in terms of direct and super-exchange interactions as

$$E(F) = B + 2E_d$$
$$E(A_1) = B + E_d + 2E_{se}$$
$$E(A_2) = B$$
$$E(A_3) = B + E_d + E_{se}$$

from which E_d and E_{se} can be obtained as a function of a_0. These are given in table 2, where E_{se} is $\sim$30% greater than and $E_d\sim$50% less than the bulk values at the monolayer lattice constant.

The occupied densities of states of the A_1 alignment over the first 12 eV, shown in figure 1, indicates further close similarities between 2D and 3D NiO. The upper valence band, $\sim$4.8 eV wide, is essentially O(p) with only a minor contribution from d_{xy} states at lower energies and negligible Ni weight at the upper edge. As in the bulk, the conduction band edge (not shown here) consists largely of d_{z^2} and $d_{x^2-y^2}$ states, so that the (100) monolayer is likewise predicted to be a p $\rightarrow$ d charge-transfer insulator. The Ni d states occur $\sim$1 eV below the O(p) band and are dispersed over $\sim$4.5 eV in three distinct sub-bands, with

$$\varepsilon(d_{z^2})_\alpha/\varepsilon(d_{x^2-y^2})_\alpha < \varepsilon(d_{xz})_\alpha/\varepsilon(d_{yz})_\alpha\varepsilon(d_{xy})_\alpha < \varepsilon(d_{xz})_\beta/\varepsilon(d_{yz})_\beta\varepsilon(d_{xy})_\beta$$

as in the bulk. This is in marked contrast to the crystal-field splitting,

$$\tilde{\varepsilon}(d_{xz})/\tilde{\varepsilon}(d_{yz}) < \tilde{\varepsilon}(d_{z^2}) < \tilde{\varepsilon}(d_{xy}) < \tilde{\varepsilon}(d_{x^2-y^2})$$

which suggests that, as in the bulk, the single particle spectrum is determined to a large extent by the on-site Coulomb and exchange terms. The DOS for the A_2, A_3 and F alignments are very similar except for very minor differences in the individual sub-band widths which result from slightly different orthogonality constraints on the total wavefunctions.

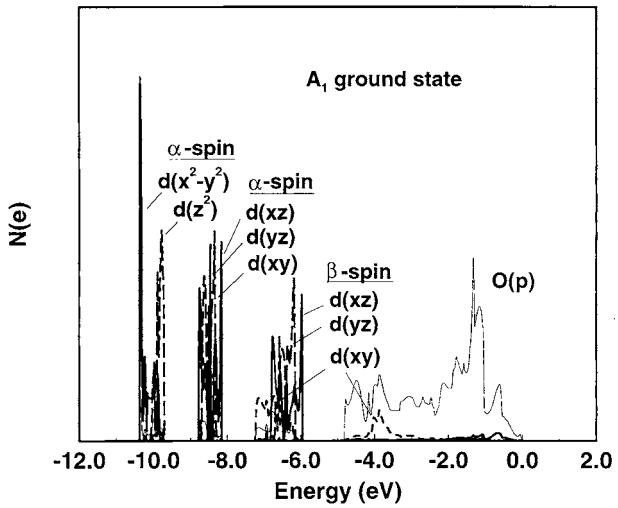

Figure 1. Valence band DOS of the A_1 ground state.

Table 2. Comparison of the direct and super-exchange interaction energies, E_d and E_{se} (meV) as a function of a_0 (Å) for the ground and $e_4\, d_{xy} \rightarrow d_{z^2}$ excited states.

	Ground state		Excited state	
a_0 (Å)	$-E_d$	$-E_{se}$	$-E_d$	$-E_{se}$
3.9	0.536	13.507	8.711	—
4.0	0.838	10.779	8.087	10.065
4.1	0.923	8.587	7.253	7.794
4.2	0.984	6.866	6.593	6.040
4.2646	0.988	5.947	6.201	5.120
4.3	0.985	5.529	5.971	4.652
4.5	0.940	3.661	4.963	2.748
5.0	0.833	1.413	3.567	0.676

3.2. d → d excited states

The lowest energy electronic excitations from the ground state in NiO correspond to orbitally forbidden ($\Delta l = 0$) local d → d transitions, or Frenkel excitons, which have been observed in both the optical [31, 32] and electron energy loss (EEL) [17, 33–36] spectra. We have obtained variationally minimized solutions corresponding to $e_1\, d_{xy} \rightarrow d_{z^2}$ and $d_{xy} \rightarrow d_{x^2-y^2}$ states, to the spin-forbidden $d_{x^2-y^2} \rightarrow d_{z^2}$ state and the two-electron $d_{xy}/d_{yz} \rightarrow d_{z^2}/d_{x^2-y^2}$ excited state for the F alignment at the minimum energy lattice constant of 4.0 Å. The corresponding excitation energies derived from direct total energy differences with respect to the ground state are listed in table 3. We have also obtained converged e_2–e_4 solutions for $d_{xy} \rightarrow d_{z^2}$ excited states for the F alignment (table 4) and e_4 solutions for the three other spin alignments, all for values of the lattice constant from 3.9 to 5.0 Å (table 5). These states remain highly ionic, high spin, insulating with changes in the ionic charges, 3d populations and local spin moments of ∼1%, ∼0.2% and ∼0.6% respectively.

For the e_4 states the differences in energy between the four spin alignments decrease rapidly with a_0, and are broadly similar in magnitude to the ground state. However, an important

Table 3. e_1 and e_0 d → d excitation energies (eV) for the F alignment at a lattice constant of 4.0 Å.

Excitation	e_1	e_0
$xy \rightarrow z^2$	1.178	1.161
$xy \rightarrow x^2 - y^2$	1.110	1.093
$x^2 - y^2 \rightarrow z^2$	1.856	1.839
$xz/yz \rightarrow z^2/x^2 - y^2$	1.809	1.792

Table 4. $d_{xy} \rightarrow d_{z^2}$ excitation energies (eV/Ni atom) as a function of a_0 (Å) for the e_1, e_4 and e_0 F spin states. E_{int} is the interaction energy (eV).

a_0 (Å)	e_1	e_2	e_3	e_4	E_0	E_{int}
3.9	1.118	1.137	1.150	1.168	1.104	0.064
4.0	1.178	1.193	—	1.218	1.161	0.057
4.1	1.227	1.240	1.249	1.260	1.215	0.045
4.2	1.269	1.280	1.287	1.296	1.259	0.037
4.2646	1.292	1.302	1.308	1.316	1.283	0.033
4.3	1.304	1.313	1.319	1.327	1.296	0.031
4.5	1.359	1.365	1.370	1.375	1.353	0.022
5.0	1.456	1.458	1.460	1.463	1.455	0.008

Table 5. Energies (meV/Ni) of the e_4 $d_{xy} \rightarrow d_{z^2}$ excited states of the A_3, F and A_2 configurations relative to A_1 as a function of a_0 (Å).

a_0 (Å)	A_3	F	A_2
3.9	—	17.323	34.747
4.0	10.065	12.161	28.335
4.1	7.794	8.390	22.335
4.2	6.040	5.474	28.660
4.2646	5.120	4.074	16.476
4.3	4.652	3.352	15.294
4.5	2.748	0.538	10.463
5.0	0.677	−2.222	4.911

difference is that unlike the ground state, the relative stability of the spin alignments in the fully saturated (e_4) $d_{xy} \rightarrow d_{z^2}$ excited state varies with a_0, as shown in table 5. Up to 4.1 Å the order is that of the ground state; from 4.2 to 4.5 Å F is more stable than A_3 and at 5.0 Å and above the order is $F < A_1 < A_3 < A_2$. However, as shown later, for values of a_0 in excess of ∼4.5 Å a single determinant description of the NiO(100) monolayer breaks down, so that the differences in energy between the spin alignments in this region are of limited significance.

For the ferromagnetic alignment we have obtained converged solutions for the full range of $d_{xy} \rightarrow d_{z^2}$ excited states, from which the corresponding excitation energies can be calculated from *direct* differences. These are listed in table 4. We have obtained values for the energy of the isolated excitation, e_0, from a non-linear regression of the e_1–e_4 excitation energies as a function of concentration, and from this the total interaction energy, E_{int}, of the excitations in the e_4 state. As shown in table 4, E_{int} is found to be small, ranging from 0.06 eV at 3.9 Å to 0.01 eV at 5.0 Å. Since it is unlikely that the interaction of d → d excited states depends strongly on the spin arrangement we have used E_{int} to obtain values of e_0 for the A_1, A_2 and A_3 states listed in table 6. Similarly, we have corrected the excitation energies given in table 3.

Table 6. Comparison of the $e_0\, d_{xy} \rightarrow d_{z^2}$ excitation energies (eV) as a function of a_0 (Å) for the A_1, A_2, A_3 and F spin alignments.

a_0 (Å)	A_1	A_2	A_3	F
3.9	1.114	1.120	—	1.104
4.0	1.170	1.176	1.169	1.161
4.1	1.223	1.226	1.222	1.215
4.2	1.266	1.270	1.265	1.259
4.2646	1.290	1.294	1.289	1.283
4.3	1.303	1.306	1.302	1.296
4.5	1.359	1.361	1.358	1.353
5.0	1.459	1.460	1.458	1.455

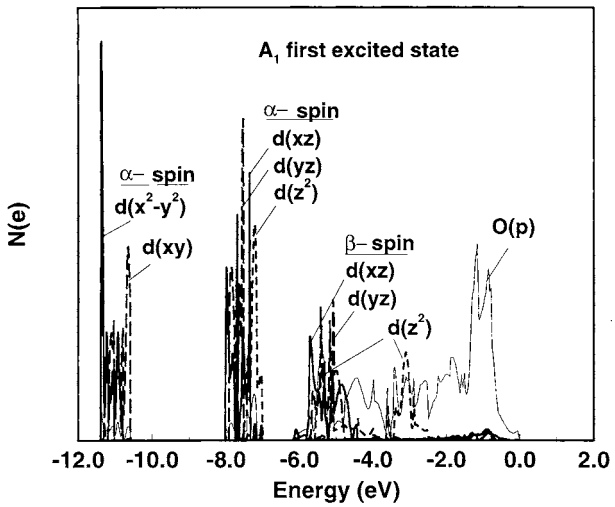

Figure 2. Valence band DOS of the $e_4A_1\, d_{xy} \rightarrow d_{z^2}$ excited state.

Assuming that the relative energies of A_1, A_2, A_3 and F can be written to a first approximation in terms of direct and super-exchange interactions, as before, we obtain values of E_d and E_{se} for the $e_4\, d_{xy} \rightarrow d_{z^2}$ excited state. They are given in table 2 which shows that while the magnitude and variation of the super-exchange energy, E_{se}, are very similar in the ground and excited states, the direct spin–spin energy is quite different in three important respects. The excited state value of E_d is roughly an order of magnitude greater than the ground state value; it decreases monotonically and fairly rapidly with a_0, unlike the ground state value which is slowly varying with a maximum at ∼4.265 Å, and above ∼4.1 Å it is greater than E_{se}.

$d_{xy} \rightarrow d_{z^2}$ excitation leads to an expected re-ordering of the single particle spectrum. However, as figure 2 shows, in other respects, the density of occupied states is remarkably similar to that of the ground state. In the $e_4\, d_{xy} \rightarrow d_{z2}\, A_1$ excited state, which, again, is typical of the other spin alignments, the minority spin d states overlap the lower part of the O(p) band, which is broadened to ∼6 eV, but there is still negligible weight of Ni states at the valence band (upper) edge, so that the p → d charge-transfer character is retained. The gap between the α- and β-spin projections of the doubly occupied states remains much the same, while that between the two bands widens from ∼1.5 eV to ∼3.5 eV.

3.3. First ionized state

The removal of an electron from a fully symmetric NiO(100) monolayer in whatever spin alignment leads to conducting states of essentially $d^8\underline{L}$ character, exactly as suggested by the ground state DOS, where the unpaired electron/hole is delocalized over the O sites, no matter what starting electronic configuration is chosen. As reported previously for the bulk [14, 15], the removal of this symmetry constraint allows the electronic configuration to relax to non-degenerate *insulating* states of *lower* energy in which the unpaired electron/hole is localized in a p_π orbital at a *single* O site. In addition to A_1 we have examined the F alignment in some detail to see whether there are any indications that a self-trapped hole might destroy the local Ni spin alignment to form spin polarons of the de Gennes type [37]. Unlike the A_1^+ hole state, for which there is a single spin configuration, there are two F^+ states, in which the spin of the unpaired electron is ferromagnetic (f) or antiferromagnetic (a) to the lattice spins. We refer to these as $F^+(f)$ and $F^+(a)$. In the localized hole state, the relative stability of the A^+ and F^+ alignments is

$$F^+(f) > A_1^+ > F^+(a)$$

with differences in energy of 0.030 eV and 0.192 eV respectively, which suggests that local A_1 order in the NiO(100) monolayer is destroyed for hole concentrations $\geqslant$0.25 hole/Ni. Mulliken population analyses indicate that in both the $F^+(f)$ and A_1^+ states $\sim$90% of the hole density is localized at a single O site with a moment of $\sim 0.9\ \mu_B$ but with no significant change in local moments at the cation sites.

Further insight into the nature of the first ionized state is contained in both the valence and conduction band DOS. Figure 3(a) shows a comparison of the valence band DOS of the A_1 ground and first ionized states. The lower panel shows that while the DOS that are projected onto the oxygen hole site and indicated as p_σ and p_π, corresponding to the doubly and singly occupied orbitals respectively, are shifted to lower energy as a result of the reduced on-site Coulomb repulsion, the remaining states are largely unaffected. Localization of a hole at a single O site also leads to the creation of a narrow band of unoccupied O(p) states at the top of the valence band, with only minimum changes at the conduction band edge, as shown in figure 3(b), and reported previously for bulk NiO [15]. This is the exactly equivalent to the changes in the oxygen K-edge spectra obtained originally by Kuiper *et al* [7] for $Li_xNi_{1-x}O$, where the energy between the extrinsically controlled unoccupied O(p) states and the conduction band edge approximates the band gap in NiO. We have estimated the band gap, E_g, as a function of a_0 in this way and compare these with values obtained directly from total energy differences in section 3.5.

3.4. First electron addition state

Our interest here relates largely to the stability of charge transfer states reported in the next section, so that our calculations are confined to the F arrangement, for which there is a single spin configuration, with the added electron anti-parallel to the lattice spin. As in the case of the first ionized state, the addition of an electron to a fully symmetric lattice leads to a conducting state of essentially d^9 character, as suggested by the ground state DOS, where the additional electron is delocalized over both Ni and O sites. Once again, the removal of this symmetry constraint allows the electronic configuration to relax to a non-degenerate *insulating* state of *lower* energy in which $\sim$80% of the added electron density is localized in a d_{z^2} orbital at a *single* Ni site with a localization energy of 2.76 eV. The local moment at this site is reduced to $\sim 1\ \mu_B$ with no significant changes to the moments at the other cation sites, as in the case of the self-trapped hole.

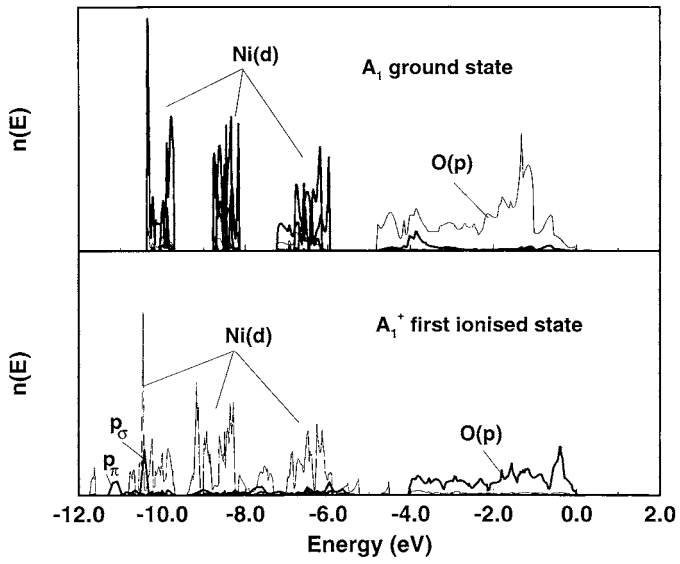

(a)

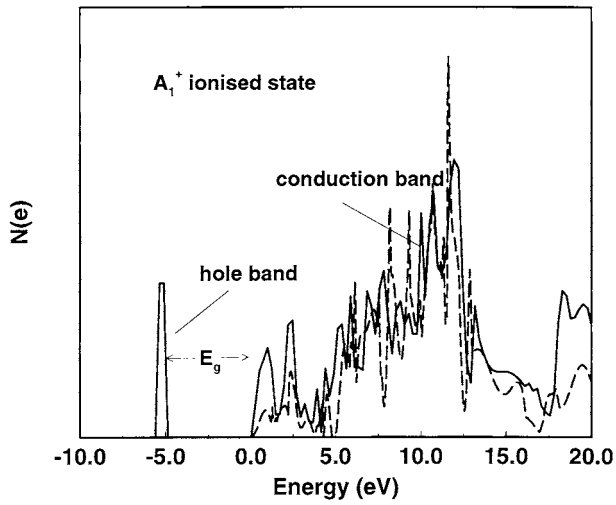

(b)

Figure 3. (a) Comparison of the valence band DOS of the A_1 ground and A_1^+ ionized states. (b) Unoccupied O(p) DOS of the A_1^+ ionized state (dashed line is the O(p) conduction band DOS of the ground state).

3.5. Charge transfer states

There have been several reports of Hartree–Fock calculations of excitonic states in insulators, notably the alkali halides, MgO, SiO_2 and Li_2O [38], but none, as far as we are aware for NiO, or of fully periodic calculations. We have confined our attention to the computationally more convenient F alignment and obtained variationally minimized solutions for the $e_4\, p_z \rightarrow d_{z^2}$ charge transfer state (Ni^+O^-) as a function of a_0 in both triplet and singlet spin states, that is

to say, configurations of the type

$$\mathrm{Ni(d^9)}_\alpha\mathrm{O(p^5)}_\alpha \text{ and } \mathrm{Ni(d^9)}_\alpha\mathrm{O(p^5)}_\beta.$$

These can be viewed as fully condensed, Mott–Wannier (MW) exciton states, so that in $\mathrm{Ni(d^9)}_\alpha\mathrm{O(p^5)}_\alpha$ the excited electron is β spin (which it must be) and the hole β spin giving a triplet exciton. The corresponding formation energies are obtained from *direct energy differences* between the ground and charge transfer states and are *lower bounds* to the optical band gap. They are given in table 7, which shows that the triplet state is the lower of the two and that formation energies decrease rapidly with a_0. The reason for this rapid decrease is evident from figure 4, which shows that above ∼5.2 Å the ground and charge transfer states cross, indicating that the lowest energy asymptotic UHF solution converges to $(\mathrm{Ni^+O^-})$ rather than $(\mathrm{Ni^{2+}O^{2-}})$. Figure 4 also suggests that a single determinant description of the wavefunction breaks down for values of a_0 in excess of ∼4.5 Å, beyond which the ground state involves a substantial mixing of $(\mathrm{Ni^+O^-})$ and $(\mathrm{Ni^{2+}O^{2-}})$ configurations. As shown in figure 5, charge transfer leads to a re-ordering of the highest occupied levels, with the minority spin d states now dominating the valence band edge and the majority of O(p) states now dispersed well below the doubly occupied d bands. The gap between the α and β doubly occupied d bands has virtually closed, while that between the two α bands has widened to ∼6 eV.

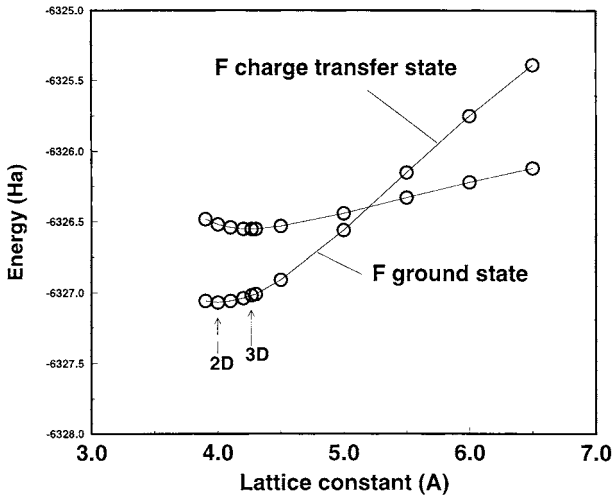

Figure 4. Comparison of the total energies (Ha) of the F ground and e_4 charge transfer states as a function of a_0 (Å).

We have obtained converged solutions for the triplet e_1 charge transfer state, i.e. a single MW exciton per 2 × 2 unit cell, but only for contractions of the appropriate $\mathrm{Ni^+}$–$\mathrm{O^-}$ distance greater than ∼0.2 Å, with no evidence of self-trapping, i.e. a local minimum in the total energy as a function of $d(\mathrm{Ni^+}$–$\mathrm{O^-})$. However, the variation of the total energy with $d(\mathrm{Ni^+}$–$\mathrm{O^-})$, for $d(\mathrm{Ni^+}$–$\mathrm{O^-}) > 0.2$ Å, is extremely smooth, which has enabled us to obtain extrapolated values of the energy of the triplet e_1 charge transfer state at zero contraction using a non-linear regression. These are listed in table 8 as the e_1 formation energies, together with the e_4 values, which were obtained directly, and the band gap, E_g, obtained from unoccupied O(p) levels in the $\mathrm{F(f)^+}$ ionized state. The difference between the e_1 and e_4 formation energies, E_{int}, which remains fairly constant at ∼2 eV, indicates that there is a strong attractive interaction between excitons leading to condensation. E_g and the e_1 and e_4 exciton formation energies are also plotted as a function of a_0 in figure 6.

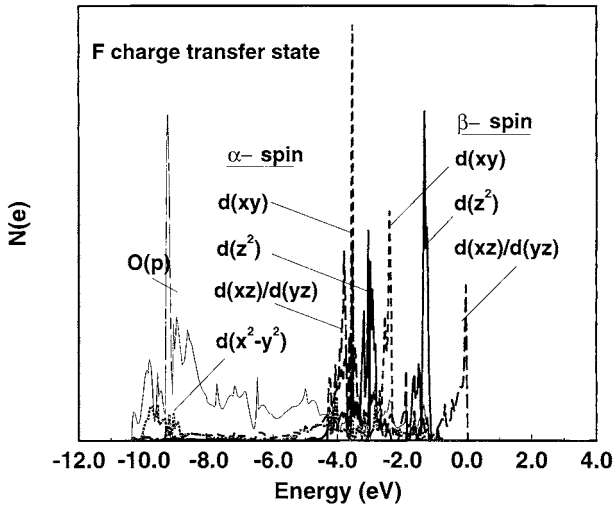

Figure 5. Valence band DOS of the e_4 F charge transfer state.

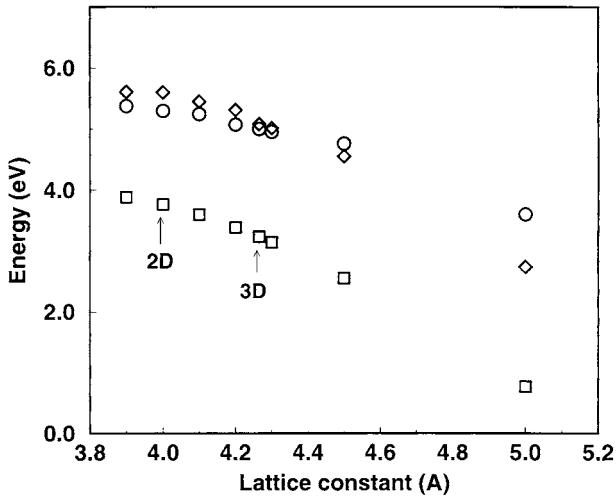

Figure 6. Comparison of E_g (circle) and e_1 (diamond) and e_4 (square) MW exciton formation energies as a function of a_0 (Å).

4. Discussion

4.1. Electronic structure of the ground state

Despite a decrease in coordination from 6 to 4 leading to a reduction of ∼8% in the Madelung potential, UHF calculations find the ionicity of monolayer NiO(100) to be substantially that of bulk crystal in all four spin configurations of the ground state considered here. Elementary considerations based on a simple Born model suggest a lattice constant of ∼5% less than the bulk value, which compares with our value of ∼6.1% from direct energy minimization of the total energy. As might have been predicted from a previous Brandow analysis of the bulk, which deduced a value of ∼0.05 eV for D_q [10], the influence of the crystal field is

Table 7. Comparison of the formation energies (eV/Ni) of the e_4 triplet and singlet excitonic states from the ferromagnetic ground state as a function of a_0 (Å). $E_{t/s}$ is the corresponding triplet–singlet splitting (eV/Ni).

a_0 (Å)	Triplet	Singlet	$E_{t/s}$
3.9	3.883	4.230	0.347
4.0	3.765	4.049	0.284
4.1	3.596	3.829	0.233
4.2	3.385	3.576	0.191
4.2646	3.230	3.398	0.168
4.3	3.139	3.296	0.157
4.5	2.506	2.613	0.107
5.0	0.776	0.820	0.044

Table 8. Comparison of the formation energies (eV/exciton) of the e_1 and e_4 triplet excitonic states, the interaction energy, E_{int}, the energy of the isolated exciton, e_0, the gap in the unoccupied DOS of the first ionized state, E_g, and the exciton condensation energy, E_{cond}, as a function of a_0 (Å).

a_0 (Å)	e_1	e_4	E_{int}	E_g
3.9	5.6	3.883	1.7	5.4
4.0	5.6	3.765	1.8	5.3
4.1	5.5	3.596	1.9	5.2
4.2	5.3	3.385	1.9	5.1
4.2646	5.1	3.230	1.8	5.0
4.3	5.0	3.139	1.9	5.0
4.5	4.6	2.506	2.0	4.8
5.0	2.7	0.776	1.9	3.6

minimal in determining the ground state configuration which is identical to that of the bulk, i.e. $[(\mathrm{d}_{xz})^2(\mathrm{d}_{yz})^2(\mathrm{d}_{xy})^2(d_{z^2})^1(d_{x^2-y^2})^1]$. The reduced Madelung potential and change in the valence band width open a gap of $\sim$1 eV between the minority spin Ni d band and the O p band, as shown in figure 1, but in all other respects the single particle spectrum resembles that of the bulk. The latter, in fact, suggests that a simple Brandow-like analysis may not be applicable to the (100) monolayer. Such an analysis, for example, finds

$$\varepsilon(\mathrm{d}_{x^2-y^2})_\alpha - \varepsilon(\mathrm{d}_{z^2})_\alpha = 16.56\ D_q \approx 0.8\ \mathrm{eV}$$

and whether the bulk value for D_q, or a slightly reduced value, which accounts for the actual geometry of the monolayer, is used, the splitting is an order of magnitude larger than the energy difference between the calculated levels at the Γ point (0.8 eV versus 0.08 eV). A simplifying feature of Brandow analysis is that U, U' and J are assumed to be the same for all d states, which might be an acceptable approximation for $[(\mathrm{d}_{xz})^2(\mathrm{d}_{yz})^2(\mathrm{d}_{xy})^2(\mathrm{d}_{z^2})^1(\mathrm{d}_{x^2-y^2})^1]$ in the highly symmetric $\mathrm{O_h}$ environment of the bulk, but not the more asymmetric $\mathrm{D_{4h}}$ symmetry of the (100) monolayer. What is clear from general considerations, however, is that the majority spin states will be lower in energy than the minority spin states by virtue of increased exchange interactions, and that the singly occupied states will be lower than the doubly occupied states by virtue of reduced Coulomb interactions, which is exactly what UHF calculations find.

4.2. Magnetic structure of the ground state

The relative energies of the four spin arrangements are as expected, $\mathrm{A_1} < \mathrm{A_3} < \mathrm{F} < \mathrm{A_2}$, for the range of a_0 up to 4.5 Å, with the magnitudes of the E_d (-0.54 meV to -0.94 meV) and E_{se}

(−13.51 meV to −3.66 meV) to be compared to the bulk values of −1.5 meV and −7.0 meV respectively. In the ground state E_d derives from the *direct* in-plane (σ) interaction of singly occupied $d_{x^2-y^2}$ orbitals and weaker out-of-plane (π) interaction of d_{z^2} orbitals *of like spin* on Ni^{2+} ions which are aligned along [011] in the (100) monolayer. For neither of the two orbitals is this a favourable configuration for overlap. Furthermore, in the bulk both d_{z^2} and $d_{x^2-y^2}$ orbitals contribute to direct in-plane interactions leading to a value of $\tilde{E}_d$ which is ∼50% greater than the corresponding monolayer value. E_{se}, on the otherhand, derives essentially from the *indirect* interaction of $d_{x^2-y^2}$ orbitals *of opposite spin*, on Ni^{2+} ions aligned (010) in the (100) monolayer, which is the optimum configuration for Ni–O overlap. Furthermore, since for a charge transfer insulator such as NiO, $E_{se} \propto t^4/E_g^3$, where t is the hopping integral and E_g the band gap, the substantially increased value of E_g for the monolayer is largely responsible for the 50% reduction of E_{se} at $a_0 = 4.0$ Å which in turn should have a major effect on the magnetic properties of the monolayer, notably the Néel temperature, T_N. While there is, of course, no direct evidence for this, Alders *et al* [4] have reported a substantial variation of T_N, with the thickness of thin overlayers of NiO grown on MgO(100). An important point here is that our interest in this paper is primarily in the *changes* in the direct and superexchange coupling energies, as between the bulk and the monolayer, the ground and excited state and as a function of lattice constant, and not their absolute values, the reliability of which is the subject of continuing investigation [39, 40].

4.3. d–d excitations

We have examined the d → d excited states in some detail with three objectives in mind. The first is to determine whether excitation energies obtained by *direct* comparison with the ground state energy are in qualitative agreement with experimental values reported for the bulk and {100} surface [18, 31–36] and with previous post-Hartree–Fock calculations [18–20] for embedded NiO_6^{10-} and NiO_5^{8-} clusters. Second, we have sought to investigate the local nature of d → d excitations in NiO; and third, we have wished to investigate the magnetism of these excited states, for general considerations suggest that the direct spin–spin interaction, E_d, for the $e_4\, d_{xy} \rightarrow d_{z^2}$ excited state should be appreciably greater than that for the ground state as a result of the overlap of *singly occupied* nearest neighbour d_{xy} orbitals.

Our estimates of 1.16 eV and 1.09 eV for the $d_{xy} \rightarrow d_{z^2}$ and $d_{xy} \rightarrow d_{x^2-y^2}$ excitations respectively of the unsupported {100} monolayer compare with experimental values of (1.05 eV–1.16 eV) [18, 31–36], which have been widely assigned to the $^3T_{2g}(t_{2g} \rightarrow e_g)$ excitation in the bulk, and with calculated values of (0.86 eV–1.04 eV) [18] and 0.79 eV [19] for the $^3T_{2g}$ state of an embedded NiO_6^{10-} cluster. They may also be compared with the 0.6 eV excitation detected by EELS [18, 35, 36], which has been assigned to the $d_{xy} \rightarrow d_{z^2}(^3E)$ state at the {100} surface of NiO on the basis of calculations for the NiO_5^{8-} cluster which predict energies of (0.54 eV–0.65 eV) [18] and 0.46 eV [20] for this state, and with energies of (0.86 eV–1.00 eV) [18] and 0.83 eV [20] which are predicted for the $d_{xz} \rightarrow d_{x^2-y^2}(^3B_2)$ state. Similarly, our energy of 1.79 eV for the two-electron $d_{xz}d_{yz} \rightarrow d_{z^2}d_{x^2-y^2}$ excitation compares with experimental values of (1.79 eV–1.95 eV) [18, 32–34], which have been assigned to the bulk $^3T_{1g}$ state, and with cluster values of (1.50 eV–1.81 eV) [18] and 1.40 eV [20]. EELS energies of (1.6 eV–1.63 eV) [18, 35, 36] have been assigned to the corresponding {100} surface state, while cluster calculations predict values of (1.11 eV–1.30 eV) [18] and 1.04 eV [20] for the $^3A_2$ state and (1.22 eV–1.44 eV) [18] and 1.17 eV [20] for the ^3E state [27]. Thus our results for the spin-allowed excitations are in broad agreement with previously reported experimental and theoretical values for the bulk and {100} surface: more detailed comparisons, particularly with regard to the variation of the excitation energy with Ni coordination will be addressed elsewhere [41].

While the overall charge distributions of the d → d excited states are similar to that of the ground state, there are minor differences which lead to increases in excitation energy as a function of a_0, as indicated in tables 3–5. Mulliken overlap populations of the excited states show these to be slightly more covalent than the ground state and, hence, they are stabilized with respect to the latter by this effect. However, these differences in covalency (overlap population) decrease with a_0 leading to an increase in excitation energy of ∼15% from 4.0 to 4.5 Å. Our calculated energies corresponding to multiple $d_{xy} \rightarrow d_{z^2}$ states in the F alignment, given in table 4, confirm the highly local nature of these, and by implication other d → d excited states, with an interaction energy of < 0.06 eV for the fully saturated excited state at 4.0 Å. This highly local nature is confirmed by table 6 which indicates that d → d excitations are largely independent of the spin alignment. As suggested above, the $(d_{xy})^1$ configuration of the $d_{xy} \rightarrow d_{z^2}$ excited state leads to an enhanced direct exchange interaction and this is borne out by table 2 which shows that E_d is approximately an order of magnitude greater than the ground state values. Furthermore, since E_d depends on nearest neighbour d_{xy}–d_{xy} overlap, it should decrease rapidly with a_0, which again is confirmed by table 2. The enhanced value of E_d in the excited state in turn increases the stability of the F spin alignment with respect to A_1, which, as tables 1 and 5 indicate, is stabilized by ∼8 meV at a lattice constant of 4.0 Å.

4.4. Band gap and excitons

As suggested both by previous results for the bulk [15] and the ground state valence band DOS shown in figure 1, the first ionized state of the 2 × 2 unit cell is found to be essentially $d^8\underline{L}$ with strong localization of the hole at a single O site in a p_π orbital leading to an insulating state and retention of the local Ni moments. We find the F^+ state with the spin of the unpaired electron parallel to the Ni spins to be 0.03 eV more stable than the A_1^+ state which suggests that the A_1 spin configuration is destroyed for hole densities $\geqslant$0.25 holes per formula unit and the formation of spin polarons of the type

O	Ni(↑)	O
Ni(↑)	O(↑)	Ni(↑)
O	Ni(↑)	O

for lower hole concentrations. As shown in figure 3(a) for the A_1 alignment, the valence band DOS remains largely unchanged with hole formation, apart from narrow bands of oxygen states projected on the hole site shifting to lower energy as a result of the reduced intra-atomic Coulomb repulsion. This detachment of filled O(p) states is accompanied by the formation of a narrow band of unoccupied O(p) states below the conduction band which is also substantially unchanged, as shown in figure 3(b). Attention has been drawn previously to the close parallel between the emergence of these unoccupied O(p) states on localized hole formation in Li:NiO [14] and NiO [15] and oxygen K-edge spectral changes for $Li_xNi_{1-x}O$ as a function of x reported by Kuiper *et al* [7], on the basis of which these authors deduced that holes in the mixed cation system were essentially of O(p) character. Again following Kuiper *et al* [7], it has been argued that the gap between the emergent band of unoccupied O(p) states and the conduction band edge approximates the optical/conductivity band, which for Li:NiO [14] and NiO [15] was found to be ∼4 eV, in agreement with the gap found by Kuiper *et al* [7] and that reported from optical absorption measurements [40]. Here we find a similar gap ranging from ∼5.3 eV at 4.0 Å to ∼4.8 eV at 4.5 Å (∼5.0 eV at the UHF bulk lattice constant of ∼4.265 Å) which, by direct analogy with the bulk, approximates the band gap in the NiO(100) monolayer. There are two principal effects that contribute to the difference in band gap between the bulk

and monolayer: the first, which is determined largely by the difference in Madelung potential of 8%, lowers the nickel states and raises the oxygen states resulting in a reduction in the band gap; the second is the computed decrease in the O(p) valence band width of ∼2–3 eV resulting from the decrease in O–O nearest neighbours from 12 in the bulk to four in the monolayer, which increases the band gap. We conclude that the latter dominates, leading to an increase of ∼1.5 eV for the (100) monolayer compared with the bulk.

We have been able to find variationally converged solutions for a single charge transfer exciton in a 2 × 2 unit cell at values of the lattice constant from 3.9 to 5.0 Å, but only for contractions of the Ni^{+}–O^{-} distance in excess of ∼0.2 Å, with no minimum energy lattice configuration. However, it is quite possible that a more extensive local distortion of the lattice and/or larger unit cell would lead to a stable structure. We have exploited the smooth variation of the energy as a function of the contracted Ni^{+}–O^{-} distance to obtain extrapolated values for zero distortion. As given in table 8, these values, designated e_1, vary from ∼5.6 eV to ∼4.6 eV for lattice constants in the range 3.9–4.5 Å, which is roughly 0.3 eV less than the corresponding values of E_g. Thus, as figure 6 illustrates further, e_1 is found to be remarkably close to E_g despite their estimation by quite different procedures. Hüfner [5] has pointed out that explanations of the value of the band gap and descriptions of the edge states of NiO (and other magnetic chalcoginides) have played a central rôle in understanding its electronic structure, and here we suggest that our two quite different approaches to calculating the band gap, one directly from the total energies of the ground and charge-transfer states, the other from the eigenvalues of the first ionized state, re-affirm the charge-transfer nature of the optical gap, in the (100) monolayer at least, and support a value close to 5.5 eV at the minimum energy lattice constant. The steepest increase in the optical absorption coefficient of bulk NiO occurs over a range of ∼1.2 eV, from ∼3.1 eV to ∼4.3 eV [42], which, in the absence of impurity and lattice defect levels, might reasonably be interpreted in terms of the formation of excitonic states below the band gap. In view of the close similarities between the bulk and (100) monolayer, similar excitonic states might also be expected to occur in the latter. This is confirmed by our variationally converged solutions for the $d^8p^6 \rightarrow d^9p^5$ charge transfer state in both triplet and singlet spin configurations, which, as we have suggested earlier, can be viewed as a fully condensed Mott–Wannier excitonic state. The energies of these states vary from ∼3.9 eV above the ground state at a lattice constant of 3.9 Å to ∼2.5 eV at 4.5 Å, i.e. roughly 1.7 eV below the band gap obtained from the unoccupied O(p) DOS of the localized hole state. Furthermore, the direct differences between e_1 and e_4 show that unlike the (repulsive) interaction between Frenkel excitons, which we estimate to be less than 0.01 eV/exciton, there is an appreciable attractive interaction between charge transfer excitons of a largely Coulombic nature, leading to an estimated condensation energy of ∼2 eV/exciton, which, again, supports the notion that the lower edge of the bulk absorption coefficient derives from associated charge-transfer excitonic states.

As in the case of d → d excitonic states, the energies of charge transfer states for the bulk and {100} surface have also been estimated from cluster calculations [20] against which the present estimates can be compared. Our value of 5.3 eV for the triplet e_1 exciton at 4.2 Å compares with energies of 7.63 eV and 5.29 eV reported by Geleijns *et al* [20] for the bulk (NiO_6^{10-}) and {100} surface (NiO_5^{8-}) respectively, at a lattice constant of 4.164 Å. However, such comparison between the two sets of calculations must be treated with caution, for we find the lowest energy excitation to be $p_z \rightarrow d_{z^2}$, whereas the (NiO_5^{8-}) cluster calculations considered electron transfer to $d_{x^2-y^2}$. Furthermore, the reported cluster calculations suggest a reduction in the band gap at the {100} surface compared with the bulk, whereas the present calculations find an increase in the band gap of the unsupported {100} monolayer compared with the bulk.

5. Conclusions

The overall conclusion of this study is that the UHF ground and excited state properties of the NiO(100) monolayer are not drastically different from those of the bulk [10], but present interesting features resulting from the reduction in dimensionality and different ordering of the d orbitals. Specifically, this study concludes that:

(i) the NiO(100) monolayer has a highly ionic, insulating $[(d_{xz})^2(d_{yz})^2(d_{xy})^2(d_{z^2})^1(d_{x^2-y^2})^1]$ configuration, with a minimum energy lattice constant, a_0, of 4.0 Å.

(ii) The valence band DOS resembles closely that of the bulk with a majority weight of O(p) states at the upper edge leading to a charge-transfer system. The Ni d states occur ∼1 eV below the O(p) band and are dispersed over ∼4.5 eV in three distinct sub-bands, with $\varepsilon(d_{z^2})_\alpha/\varepsilon(d_{x^2-y^2})_\alpha < \varepsilon(d_{xz})_\alpha/\varepsilon(d_{yz})_\alpha\varepsilon(d_{xy})_\alpha < \varepsilon(d_{xz})_\beta/\varepsilon(d_{yz})_\beta\varepsilon(d_{xy})_\beta$.

(iii) The relative stability of the four spin alignments examined is in the order antiferromagnetic > ferrimagnetic > ferromagnetic > fully frustrated with differences in energy of 10.779 meV, 10.017 meV and 1.675 meV respectively.

(iv) Differences in the direct spin–spin and superexchange coupling energies, E_d and E_{se}, between the monolayer and the bulk have been found. They are related to the specific orbital contributions to these energies and to the increased band gap of the monolayer.

(v) For ferromagnetic alignment at a_0 the energies of the one-electron $d_{xy} \rightarrow d_{z^2}$, $d_{xy} \rightarrow d_{x^2-y^2}$ and spin-forbidden $d_{x^2-y^2} \rightarrow d_{z^2}$ excited states and two electron $d_{xy}/d_{yz} \rightarrow d_{z^2}/d_{x^2-y^2}$ excited state are calculated to lie 1.16 eV, 1.09 eV, 1.84 eV and 1.79 eV respectively above the ground state. These may be compared to the values assigned to the bulk (1.05 eV–1.95 eV) and {100} surface (0.57 eV and 1.62 eV) from optical and EEL spectra and previous high-level cluster calculations which report bulk and surface energies of (1.00 eV–1.81 eV) and (0.54 eV–1.38 eV) respectively [27].

(vi) The $d_{xy} \rightarrow d_{z^2}$ excited state, and by implication the other d → d excited states, is highly localized, with an interaction energy of < 0.1 eV per excitation for the fully saturated state, independent of spin alignment. The excitation energy increases by ∼0.42 eV Å^{-1} in the range of a_0 from 3.9 to 4.5 Å as a result of the relative changes in covalency of the ground and excited states as a_0 is varied.

(vii) In the $d_{xy} \rightarrow d_{z^2}$ excited state the favourable arrangement of the nearest neighbour unpaired spins leads to values of E_d, the direct spin–spin coupling energy, which are an order of magnitude greater than the ground state values and appreciably in excess of the bulk value due to the $(d_{xy})^1$ configuration of the $d_{xy} \rightarrow d_{z^2}$ excited state. The values of E_{se}, on the other hand, remain approximately the same. This induces an increased stability of the F spin alignment with respect to A_1.

(viii) The first ionized state is essentially $d^8\underline{L}$, as it is in the bulk, with strong localization of the hole in a p_π orbital of a single O atom and retention of the local Ni moments.

(ix) The creation of holes at densities ⩾0.25 holes per NiO destroys the antiferromagnetic spin alignment and at lower densities the formation of spin polarons with ferromagnetic alignment of the Ni spins nearest neighbour to the local O moment.

(x) By direct analogy with the changes in the oxygen K-edge spectrum of $Li_xNi_{1-x}O$ as a function of x reported by Kuiper *et al* [7], the band gap in the NiO(100) monolayer is estimated to be ∼5.3 eV from the gap between the hole band and the conduction band edge at an a_0 of 4.0 Å. This value is substantially larger than in the bulk, even for equal lattice constants. The narrowing of the valence band due to the reduced oxygen coordination in the monolayer may be responsible for such an enlargement.

(xi) The first electron addition state is essentially $d^9[(d_{z^2})^2]$, with a localization energy of 2.76 eV.

(xii) The energy of a single charge-transfer excitonic state of a 2×2 unit cell is estimated to be ∼5.6 eV at a lattice constant of 4.0 Å, in close agreement with the band gap deduced from the DOS of the first ionized state (5.3 eV).

(xiii) the formation energy of the triplet $p_z \rightarrow d_{z^2}$ charge transfer state (Ni^+O^-), which can be viewed as the fully condensed charge-transfer excitonic state, is 3.78 eV at an a_0 of 4.0 Å, with the singlet state 0.28 eV higher in energy.

Finally, we conclude that the results reported here represent a useful prelude to more extensive studies of ultra-thin films and nanostructures in which the influence of the physical and chemical structure of the substrate will be examined in more detail.

Acknowledgments

WCM wishes to thank L'Université Paris Sud for the award of a Professeur Invité during the tenure of which the majority of the work reported here was completed.

References

[1] Kuhlenbeck H and Freund H J 1977 *Growth and Properties of Ultrathin Epitaxial Layers (The Chemical Physics of Solid Surfaces 8)* ed D A King and D P Woodruff (Amsterdam: Elsevier)
[2] Fujii T, Alders D, Voogt F C, Hibma T, Thole B T and Sawatzky G A 1996 *Surf. Sci.* **366** 579
[3] Hesper R, Tjeng L H and Sawatzky G A 1997 *Europhys. Lett.* **40** 177
[4] Alders D, Tjeng L H, Voogt F C, Hibma T, Sawatzky G A, Chen C T, Vogel J, Sacchi M and Iacobucci S 1998 *Phys. Rev.* B **57** 11 623
[5] Hüfner S 1994 *Adv. Phys.* **43** 183
[6] Terakura K, Williams A R, Oguchi T and Kübler J 1984 *Phys. Rev.* B **30** 4734
[7] Kuiper P, Kruizinga G, Ghijsen J, Sawatzky G A and Verweij H 1989 *Phys. Rev. Lett.* **62** 221
[8] van Elp J, Searle B G, Sawatzky G A and Sacchi M 1991 *Solid State Commun.* **80** 67
[9] van Elp J, Eskes H, Kuiper P and Sawatzky G A 1992 *Phys. Rev.* B **45** 1612
[10] Towler M D, Allan N L, Harrison N M, Saunders V R, Mackrodt W C and Aprà E 1994 *Phys. Rev.* B **50** 5041
[11] Towler M D, Allan N L, Harrison N M, Saunders V R and Mackrodt W C 1995 *J. Phys.: Condens. Matter* **7** 6231
[12] Harrison N M, Saunders V R, Dovesi R and Mackrodt W C 1998 *Phil. Trans. Roy. Soc.* A **356** 75
[13] Dovesi R, Saunders V R, Roetti C, Causà M, Harrison N M, Orlando R and Aprà E 1995 *CRYSTAL 95, User Manual* (Università di Torino and CCLRC Daresbury Laboratory)
[14] Mackrodt W C, Harrison N M, Saunders V R, Allan N L and Towler M D 1996 *Chem. Phys. Lett.* **250** 66
[15] Mackrodt W C 1997 *Ber. Bunsenges. Phys. Chem.* **101** 169
[16] Springhorn C and Schmalzried H 1994 *Ber. Bunsenges. Phys. Chem.* **98** 746
[17] deGraaf C, Broer R and Nieuwpoort W C 1997 *Chem. Phys. Lett.* **271** 372
[18] Freitag A, Staemmler V, Cappus D, Ventrice C A, Al Shamery K, Kuhlenbeck H and Freund H-J 1993 *Chem. Phys. Lett.* **210** 10
[19] deGraaf C, Broer R and Nieuwpoort W C 1996 *Chem. Phys.* **208** 35
[20] Geleijns M, deGraaf C, Broer R and Nieuwpoort W C 1999 *Surf. Sci.* **421** 106
[21] See, for example, Stoneham A M 1985 *Theory of Defects in Solids* 2nd edn (Oxford: Oxford University Press)
[22] Burke M L and Goodman D W 1994 *Surf. Sci.* **311** 17
[23] Xu C, Oh W S, Guo Q and Goodman D W 1996 *J. Vac. Sci. Technol.* A **14** 1395
[24] Guo Q, Xu C and Goodman D W 1998 *Langmuir* **14** 1371
[25] Pisani C, Dovesi R and Roetti C 1988 *Hartree–Fock Ab Initio Treatment of Crystalline Systems* (Berlin: Springer)
[26] Pople J A and Nesbet R K 1954 *J. Chem. Phys.* **22** 571
[27] Dovesi R, Causà M, Orlando R, Roetti C and Saunders V R 1990 *J. Chem. Phys.* **92** 7402
[28] Monkhorst H J and Pack J D 1976 *Phys. Rev.* B **13** 5188
[29] Brandow B H 1970 *Adv. Phys.* **26** 651
[30] Mulliken R S 1955 *J. Chem. Phys.* **23** 1833
Mulliken R S 1955 *J. Chem. Phys.* **23** 1841
[31] Newman R and Chrenko R M 1959 *Phys. Rev.* **114** 1507

[32] Propach V, Reinen D, Drenkhaln H and Müller Buschbaum H 1978 *Z. Naturforsch.* b **33** 619
[33] Cox P A and Williams A A 1985 *Surf. Sci.* **152** 791
[34] Hüfner S, Steiner P, Reinert F, Schmitt H and Sandl P 1992 *Z. Phys.* B **88** 247
[35] Fromme B, Schmitt M, Kisker E, Gorschlüter A and Merz H 1994 *Phys. Rev.* B **50** 1874
[36] Fromme B, Möller M, Anschütz Th, Bethke C and Kisker E 1996 *Phys. Rev. Lett.* **77** 1548
[37] Mackrodt W C and Williamson E-A 1997 *J. Phys.: Condens. Matter* **9** 6591
[38] See, for example, Shluger A L, Harker A H, Grimes R W and Catlow C R A 1992 *Phil. Trans. R. Soc.* A **341** 221 and references therein
[39] Moreira I D and Illas F 1997 *Phys. Rev.* B **55** 4129
[40] De Graaf, Illas F, Broer R and Nieuwpoort W C 1997 *J. Chem. Phys.* **106** 3287
[41] Mackrodt W C and Noguera C unpublished results
[42] Powell R J and Spicer W E 1970 *Phys. Rev.* B **2** 2182